

Fracture of Nano and Engineering Materials and Structures

Proceedings of the 16th European Conference of
Fracture, Alexandroupolis, Greece, July 3–7, 2006

Edited by

E. E. GDOUTOS

*Democritus University of Thrace,
Dept of Civil Engineering, Xanthi, Greece*

 Springer

A C.I.P. Catalogue record for this book is available from the Library of Congress.

ISBN-10 1-4020-4971-4 (HB)
ISBN-13 978-1-4020-4971-2 (HIB)
ISBN-10 1-4020-4972-2 (e-book)
ISBN-13 978-1-4020-4972-9 (e-book)

Published by Springer,
P.O. Box 17, 3300 AA Dordrecht, The Netherlands.

www.springer.com

Cover picture

Fracture and Delamination of Oxide: Fracture and delamination of $1\mu\text{m}$ (1×10^{-6} m)
 SiO_2 on Si with $1\mu\text{m}$ conical probe tip. Courtesy of Hysitron Inc., Minneapolis, Minnesota, USA

Printed on acid-free paper

All Rights Reserved
© 2006 Springer

No part of this work may be reproduced, stored in a retrieval system, or transmitted in any form or by any means, electronic, mechanical, photocopying, microfilming, recording or otherwise, without written permission from the Publisher, with the exception of any material supplied specifically for the purpose of being entered and executed on a computer system, for exclusive use by the purchaser of the work.

Printed in the Netherlands.

DEFECT IN ULTRA-FINE GRAINED MG-BASED ALLOYS DEFORMED BY HIGH-PRESSURE TORSION

J. Cizek, I. Prochazka, B. Smola, I. Stulikova, R. Kuzel, Z. Matej and V. Cherkaska
Faculty of Mathematics and Physics, Charles University in Prague, Czech Republic

V Holešovičkách 2, CZ-180 00 Praha 8 Czech Republic

R.K. Islamgaliev, O. Kulyasova

Ufa State Aviation Technical University, Russia

Ufa 450 000, Russia

jczek@mbox.troja.mff.cuni.cz

Applications of Mg-based alloys at elevated temperatures are limited by the low melting point of Mg. This difficulty can be overcome by an addition of rare earth elements. A number of novel promising Mg-based hardenable alloys with high creep resistance at elevated temperatures have been developed, e.g. Mg-Gd, Mg-Mn-Sc etc. Despite the favorable strength and thermal stability, a disadvantage of these alloys consists in a low ductility, which is not sufficient for industrial applications. Grain refinement is known as a way how to improve ductility. It has been demonstrated that an extreme grain size reduction can be achieved by methods based on severe plastic deformation (SPD). In the present work we used high pressure torsion (HPT), which is the most efficient in grain size reduction among the SPD-based techniques, for preparation of selected Mg-based alloys with ultra fine grained (UFG) structure. Microstructure investigations and defect studies of HPT deformed UFG Mg-based alloys are presented in this paper. The extraordinary properties of UFG materials are closely related with defects (grain boundaries, dislocations) introduced by HPT. Positron lifetime (PL) spectroscopy [1] is a well-established non-destructive technique with high sensitivity to open volume defects. It enables identification of the defect types present in the material studied and determination of defect densities. Thus, PL spectroscopy represents an ideal tool for defect studies of UFG materials. In the present work PL spectroscopy was combined with X-ray diffraction (XRD), microhardness measurements, and direct observations of microstructure by TEM.

Typical TEM image of HPT deformed Mg-10wt.%Gd alloy is shown in Fig. 1 as an example. It exhibits homogeneous UFG structure with grain size around 100 nm, mainly high-angle type grain boundaries, and high dislocation density. High number of dislocations leads to a significant broadening of XRD profiles. Two components were resolved in PL spectrum of HPT deformed Mg-10wt.%Gd alloy. Namely the free-positron component and a contribution of positrons trapped at dislocations, which represent dominant positron trapping sites. Spatial distribution of dislocations was investigated.

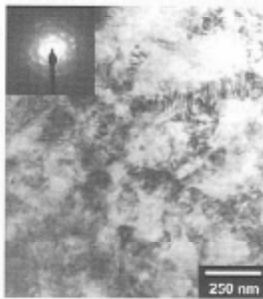


FIGURE 1. A TEM image of Mg-10wt.%Gd alloy deformed by HPT.

References

1. Hautojärvi, P., Corbel, C., In *Proceedings of the International School of Physics "Enrico Fermi", Course CXXV*, edited by A. Dupasquier, A.P. Mills, IOS Press, Varena 1995, 491-532.

DEFECT IN ULTRA-FINE GRAINED MG-BASED ALLOYS DEFORMED BY HIGH-PRESSURE TORSION

J. Čížek*, I. Procházka, B. Smola, I. Stulíková, R. Kužel, Z. Matěj, V. Cherkaska
Faculty of Mathematics and Physics, Charles University, Prague
V Holešovičkách 2, Praha 8 CZ-180 00, Czech Republic
* corresponding author e-mail: jcizek@mbox.troja.mff.cuni.cz

R.K. Islamgaliev, O. Kulyasova
Ufa State Aviation Technical University, Russia
Ufa 450 000, Russia

ABSTRACT

Applications of Mg-based alloys at elevated temperatures are limited by the low melting point of Mg. This difficulty can be overcome by an addition of rare earth elements. A number of novel promising Mg-based hardenable alloys with high creep resistance at elevated temperatures have been developed, e.g. Mg-Gd, Mg-Mn-Sc etc. Despite the favourable strength and thermal stability, a disadvantage of these alloys consists in a low ductility, which is not sufficient for industrial applications. Grain refinement is known as a way how to improve ductility. It has been demonstrated that an extreme grain size reduction can be achieved by methods based on severe plastic deformation (SPD). In the present work we used high pressure torsion (HPT), which is the most efficient in grain size reduction among the SPD-based techniques, for preparation of selected Mg-based alloys with ultra fine grained (UFG) structure. Microstructure investigations and defect studies of HPT deformed UFG Mg-based alloys are presented in this paper. The extraordinary properties of UFG materials are closely related with defects (grain boundaries, dislocations) introduced by HPT. Positron lifetime (PL) spectroscopy is a well-established non-destructive technique with high sensitivity to open volume defects. It enables identification of the defect types present in the material studied and determination of defect densities. Thus, PL spectroscopy represents an ideal tool for defect studies of UFG materials. In the present work PL spectroscopy was combined with X-ray diffraction (XRD), microhardness measurements, and direct observations of microstructure by TEM.

Introduction

Lightweight Mg-based alloys enable to increase the effectiveness in automotive and air industries and in structural applications, which leads to a lower consumption of the fossil fuels and other energetic sources. However, the applicability of magnesium alloys is limited due to their low melting temperature T_m . A failure of the construction units can happen at temperatures higher than 0.4-0.5 T_m , i.e. 100-200°C. There is a big effort in materials science to extend the applicability of Mg-alloys to higher temperatures. The particularly promising way is use of rare earth alloying elements [1]. For example Mg-Gd system represents a promising novel hardenable material with high creep resistance even at elevated temperatures [2]. Despite the favourable strength and thermal stability, a disadvantage of Mg-based alloys with rare earth elements consists in a low ductility, which is not sufficient for industrial applications. Thus, attempts to increase ductility of these alloys are highly desirable. Grain refinement is a well-known method how to increase ductility of metallic materials. Recently it has been demonstrated that ultra fine grained (UFG) metals with grain size around 100 nm can be produced by high pressure torsion (HPT) [3]. A number of UFG metals exhibit favourable mechanical properties consisting in a combination of very high strength and a sufficient ductility. For this reason, it is highly interesting to examine microstructure and physical properties of UFG Mg-based light alloys. Following this purpose, microstructure investigations of HPT deformed pure Mg and Mg-9.33wt.%Gd (Mg10Gd) were performed in the present work. A typical feature of UFG structure is very high number of lattice defects introduced by HPT. These defects influence significantly physical properties of UFG materials. Their characterisation represents, therefore, an important task in microstructure investigations of UFG materials. Positron lifetime (PL) spectroscopy was employed in present work for defect studies. It is well known that PL spectroscopy represents a well developed non-destructive technique with very high sensitivity to open-volume defects like vacancies, dislocations, etc. [4]. Thus, PL spectroscopy is an ideal tool for defects studies of UFG materials. In this work we combined PL spectroscopy with transmission electron microscopy (TEM), X-ray diffraction (XRD) and measurement of microhardness.

Experimental

The specimens of Mg (technical purity) and Mg10Gd alloy were investigated. The Mg10Gd alloy was prepared from the technical purity Mg by squeeze casting. The as-cast material was subjected to homogenization annealing at 500°C for 6 hours finished by rapid quenching. UFG samples were prepared from the as-received

Mg and the homogenized Mg10Gd alloy by HPT at room temperature up to the true logarithmic strain $\epsilon = 7$ under high pressure of 6 GPa [3]. The HPT deformed samples were disk shaped with diameter 12 mm and thickness 0.3 mm. The isochronal annealing was performed step-by-step in a silicon oil bath and a vertical furnace with protective Ar atmosphere. Each annealing step was finished by quenching and microstructure investigations at room temperature. In addition a well annealed high purity Mg (99.95%) and Gd (99.9%) were used as reference specimens.

A fast-fast spectrometer similar to that described in [5] with timing resolution 170 ps was employed in the present work. Diameter of the positron source spot was 3-4 mm and PL measurements were carried out at the centre of the studied samples. Decomposition of positron lifetime (PL) spectra into exponential components was performed using a maximum likelihood procedure [6]. The PL measurements were accompanied by theoretical calculations of positron lifetimes using the atomic superposition method (ATSUP) [7]. TEM observations were performed on the JEOL 2000 FX electron microscope operating at 200 kV. XRD studies were carried out with the aid of XRD7 and HZG4 (Seifert-FPM) powder diffractometers using Cu K_{α} radiation. The microhardness HV was measured by the Vickers method at load of 100 g applied for 10 s using the LECO M-400-A hardness tester.

Results and Discussion

The reference high purity Mg sample exhibits a single-component PL spectrum with lifetime $\tau_1 = 227$ ps, see Table 1. It exhibits a reasonable agreement with calculated Mg bulk lifetime $\tau_B^{Mg} = 233$ ps. On the other hand, PL spectrum of the as-received Mg sample (e.i. prior to HPT deformation) consists of two components listed in Table 1. The lifetime τ_1 of the shorter component corresponds to free positrons, while the longer component with lifetime $\tau_2 = 256$ ps comes from positrons trapped at defects. The lifetime τ_2 lies between the Mg bulk lifetime τ_B^{Mg} and the calculated lifetime of positrons trapped at Mg-vacancy $\tau_v^{Mg} = 297$ ps. It is typical for dislocations. A typical TEM image of the as-received Mg sample is shown in Figure 1a. Dislocation density $\rho \approx 5 \times 10^{12} \text{ m}^{-2}$ and the mean grain size of about 10 μm were estimated by TEM in this specimen. Thus, we conclude that positrons are trapped at dislocations introduced into the as-received Mg during casting and shaping. In order to check experimentally this interpretation, a technical purity Mg sample was cold rolled to thickness reduction $\epsilon = 40\%$. The second component in the cold rolled sample exhibits indeed virtually the same lifetime τ_2 (see Table 1), but significantly higher intensity due to higher dislocation density. Annealing of the as-received Mg at 280 °C for 30 min leads to a complete recovery of dislocations reflected also by a remarkable decrease of microhardness HV (the last column of Table 1). The annealed sample exhibits a single component PL spectrum with lifetime which agrees reasonably with that of the reference high purity Mg specimen. The reference high purity Gd sample exhibits a single-component PL spectrum with lifetime 201 ps. It is in very good agreement with calculated lifetime of free positrons in Gd $\tau_B^{Gd} = 204$ ps.

Table 1. Lifetimes τ_i and corresponding relative intensities I_i of the exponential components resolved in PL spectra (except of the source contribution). The intensities are normalized so that $I_1 + I_2 = 100\%$. The PL results for HPT deformed materials correspond to the centre of the sample. Microhardness values HV are shown in the last column. In case of HPT deformed samples HV in the centre and at the margin of the sample are given. The errors (one standard deviations) are given in parentheses.

Sample	τ_1 (ps)	I_1 (%)	τ_2 (ps)	I_2 (%)	HV 0.1
high purity Gd, well annealed	201.3(5)	100	-	-	
high purity Mg, well annealed	227.0(5)	100	-	-	
Mg as-received	204(4)	63(1)	256(1)	37(1)	440(40)
Mg annealed 280°C/30 min	225.3(4)	100	-	-	330(20)
Mg cold rolled $\epsilon = 40\%$	160(10)	14(4)	257(2)	86(4)	
Mg10Gd homogenized	220(4)	90.9(6)	301(9)	9.1(7)	680(30)
HPT deformed Mg	188(5)	39(1)	257(3)	61(1)	570(30)-620(30)
HPT deformed Mg10Gd	210(3)	34(2)	256(3)	66(2)	1670(40)-2330(40)

A bright-field TEM image and an electron diffraction pattern of the HPT deformed Mg specimen are shown in Figure 1b. Two different kinds of regions were observed: (i) "deformed regions" with UFG grains (100-300 nm) and high dislocation density, and (ii) "recrystallized regions" with substantially larger grains (1-5 μm) and almost free of dislocations. The presence of the "recrystallized regions" indicates an incomplete dynamic recovery of the microstructure during the HPT processing. The XRD back-reflection pattern for HPT deformed Mg sample is a superposition of isolated spots and continuous diffraction rings, which testifies co-existence of the two kinds of regions mentioned above. The sample shows a texture of (001) type. No significant broadening of XRD profiles was detected. It is because of a major contribution to the diffraction peaks comes from the "recrystallized regions" so that the "deformed regions" cannot be well characterized by XRD. The PL spectrum of the HPT deformed Mg consists of the free positron component with lifetime τ_1 and intensity I_1 and a contribution of positrons trapped at dislocations inside the "deformed regions" (lifetime τ_2 and intensity I_2), see Table 1. The HPT deformed Mg sample exhibits substantially increased hardness (see Table 1) due to hardening caused by dislocations introduced by HPT. A slight increase of microhardness from the centre of the sample towards the margins was detected. Dependence of microhardness HV on the radial distance r from the centre of the sample was

measured and is plotted in Figure 2a. The increase of microhardness from the centre of the sample towards margin reflects an increase of dislocation density. The centre of the sample exhibits the lowest dislocation density, while the highest number of dislocations can be found at the margins. Such spatial distribution of dislocations was found also in HPT deformed Cu [8] and seems to be typical for a number of HPT deformed materials. This effect occurs because strain in torsion deformation increases with the radial distance from the centre of rotation [3]. However, it should be stressed that the difference of dislocation density between the centre of the HPT deformed sample and the margins is negligible when compared with difference of dislocation density in the HPT deformed sample and the initial coarse-grained material. The increase of HV from the centre to the margin amounts $\approx 9\%$ in the HPT deformed Mg, but on average the HPT deformed sample exhibits about of 80% higher HV with respect to the annealed Mg sample.

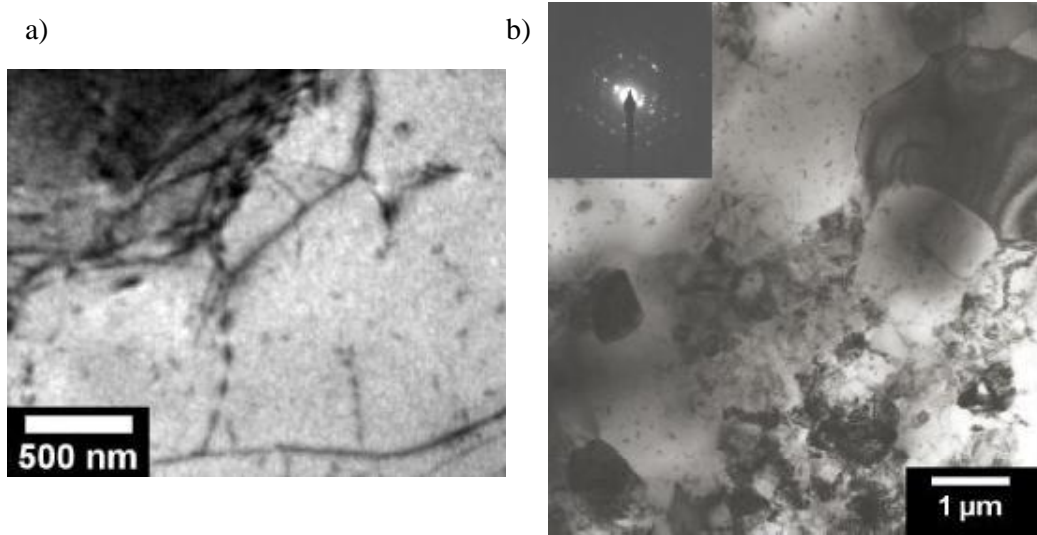


Figure 1: Bright-field TEM image of Mg sample: a) as-received b) HPT deformed.

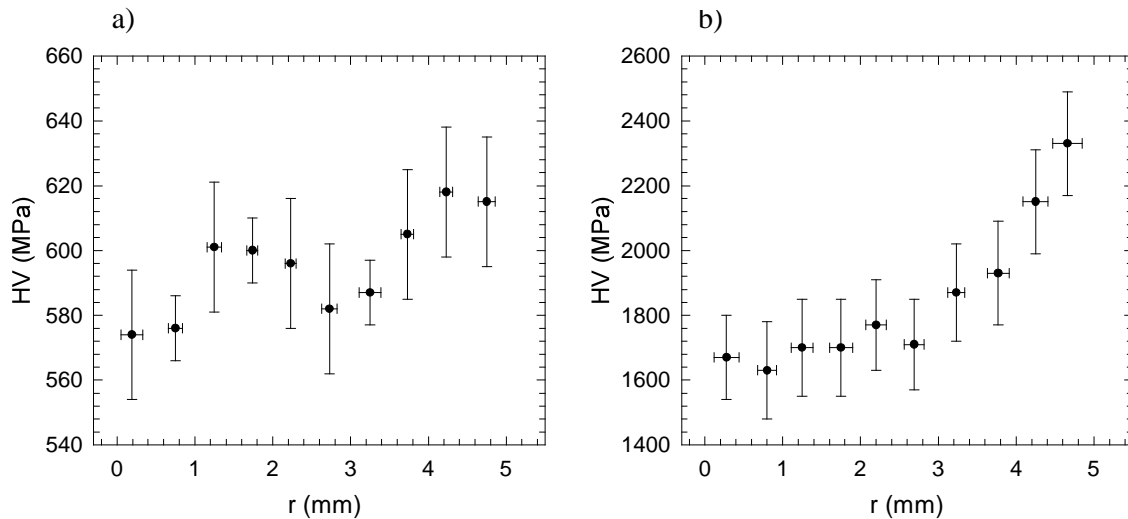


Figure 2: Microhardness HV as a function of the radial distance r from the center of the specimen a) HPT deformed pure Mg, b) HPT deformed Mg10Gd. Each point in the figures represents a mean value from 10 independent measurements at various positions in the same radial distance.

A bright-field TEM image of the homogenized Mg10Gd alloy is shown in Figure 3a. Large coarse grains were observed. The sample exhibits a low dislocation density below $\approx 10^{12} \text{ m}^{-2}$. The PL spectrum of this specimen is well fitted by two exponential components given in Table 1. The first component with the lifetime $\tau_1 < \tau_B^{\text{Mg}}$ can be attributed to free positrons, while the second one with the lifetime τ_2 comes from positrons trapped at defects. The low dislocation density in the specimen approaches the lower sensitivity limit of PL spectroscopy [4]. Therefore, positrons trapped at dislocations cannot represent a noticeable contribution to PL spectrum. The second component with the lifetime τ_2 represents a contribution of positrons trapped in quenched-in excess vacancies, which were "frozen" in the sample due to the rapid quenching. This interpretation is supported by the lifetime $\tau_2 \approx$

300 ps, which is remarkably higher than the lifetime 256 ps of positrons trapped in Mg-dislocations, but agrees well with the calculated lifetime of positrons trapped in Mg vacancy $\tau_v^{\text{Mg}} = 297$ ps. Vacancies in pure Mg become mobile below room temperature [9]. Thus, free Mg vacancies are not stable at room temperature and are quickly annealed out. Contrary to it, we observed that positrons are trapped in vacancies in the homogenized Mg10Gd sample. The explanation is that the vacancies are bound to Gd atoms. The vacancy-Gd pairs are stable at room temperature. Calculated lifetime of positrons trapped in Mg-vacancy bound to Gd atom practically does not differ from the lifetime of positrons trapped in a free Mg-vacancy [10]. Thus, a free vacancy and a vacancy-Gd pair cannot be distinguished by PL spectroscopy. Moreover, an enhanced amount of Gd in the vicinity of vacancies was proved by coincidence Doppler broadening measurements [10]. Microhardness $\text{HV} = 680 \pm 50$ MPa was measured on the homogenized Mg10Gd sample. It is in reasonable agreement with the hardness measured on this alloy after homogenization in [2].

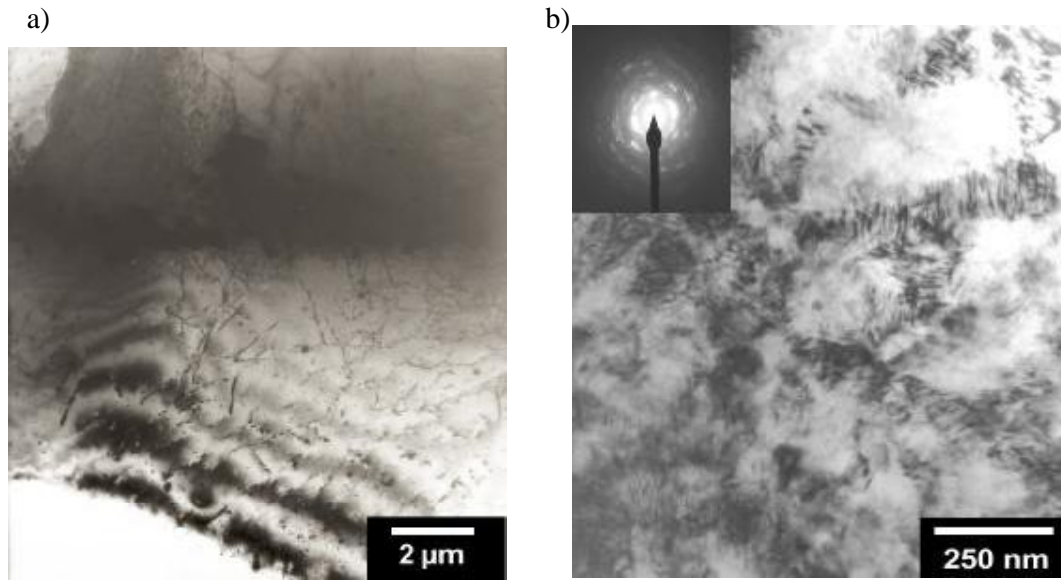


Figure 3: A bright-field TEM image of Mg10Gd alloy: a) homogenized 500 °C / 6h b) HPT deformed.

A bright-field TEM image and an electron diffraction pattern for the HPT deformed Mg10Gd alloy are shown in Figure 3b. It exhibits uniform UFG microstructure with the mean grain size about 100 nm, i.e. no dynamic recovery took place during the HPT processing. The electron diffraction pattern shows high-angle misorientation of neighboring grains. High density of homogeneously distributed dislocations was observed. A high dislocations density is reflected by a significant broadening of XRD profiles. A lower broadening of (00l) profiles with respect to other peaks indicates dominating presence of $\langle a \rangle$ dislocations with Burgers vector $\vec{b} = 1/3 \cdot a \cdot [2\bar{1}\bar{1}0]$. A weak (001) texture was found. The PL spectrum of the HPT deformed Mg10Gd alloy consists of two components, see Table 1. The first component with the lifetime τ_1 comes from free positrons, while the second component with dominant intensity comes from positrons trapped at Mg-dislocations. Similarly to HPT deformed Mg, we have found that there is an increase of dislocation density from the centre of the sample towards the margin seen by an increase of microhardness with the radial distance r from the centre of the sample, see Figure 2b. Contrary to HPT deformed fcc and bcc metals [11,12], no microvoids have been detected.

After characterization of the as-deformed microstructure, the samples were subjected to isochronal annealing in order to examine development of microstructure with increasing temperature and recovery of defects. The PL spectra of HPT deformed Mg and Mg10Gd samples consisted of the two components with lifetimes τ_1 (free positrons) and τ_2 (positrons trapped at dislocations) at all annealing temperatures. The lifetime τ_2 did not change with annealing temperature (except of statistical fluctuations) indicating that nature of positron traps remains unchanged. Therefore, in order to decrease statistical uncertainties of the fitted parameters we fixed the lifetime τ_2 to 256 ps in the final analysis of PL spectra.

The relative intensity I_2 of the dislocation component for HPT deformed Mg is plotted in Figure 4a as a function of annealing temperature. Recrystallization is seen by a pronounced decrease of I_2 because the “deformed regions” with high dislocation density and UFG structure are gradually replaced by dislocation-free recrystallized grains. As discussed above, in HPT deformed Mg this process starts already at room temperature during the HPT deformation. Indeed, a decrease of I_2 occurs already from room temperature, see Figure 4a. Recrystallization leads also to a significant softening seen by a strong decrease of HV, see Figure 5a. HV decreases mostly in the temperature range (20-140)°C, i.e. during the first stages of recrystallization. The volume fraction of the “recrystallized grains” increases with increasing temperature. It can be seen in Figure 6a which shows a bright field TEM image of HPT deformed Mg sample annealed up to 100 °C. Eventually at 200°C the sample exhibits

completely recrystallized structure shown in Figure 6b. The recrystallized sample exhibits a low dislocation density $\rho \approx 1 \times 10^{12} \text{ m}^{-2}$ and the mean grain size $\approx 5 \mu\text{m}$. The recrystallized structure remains essentially the same after annealing to higher temperatures. It is in concordance with PL and HV results. Only a minor decrease of I_2 and HV caused likely by growth of the recrystallized grains can be seen above 200 °C in Figures 4a and 5a, respectively.

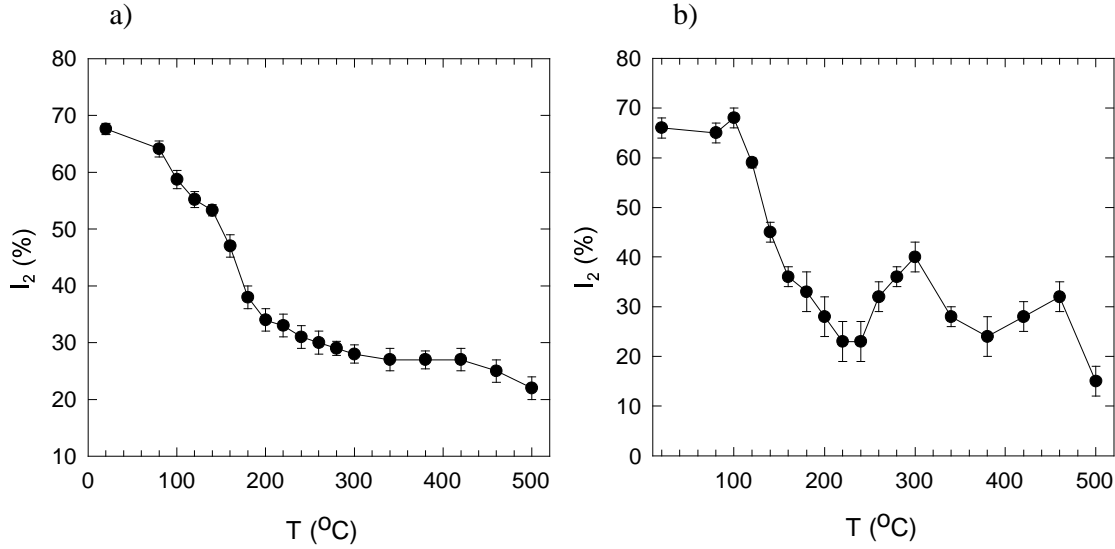


Figure 4: Temperature dependence of intensity I_2 of positrons trapped at dislocations a) HPT deformed pure Mg, b) HPT deformed Mg10Gd.

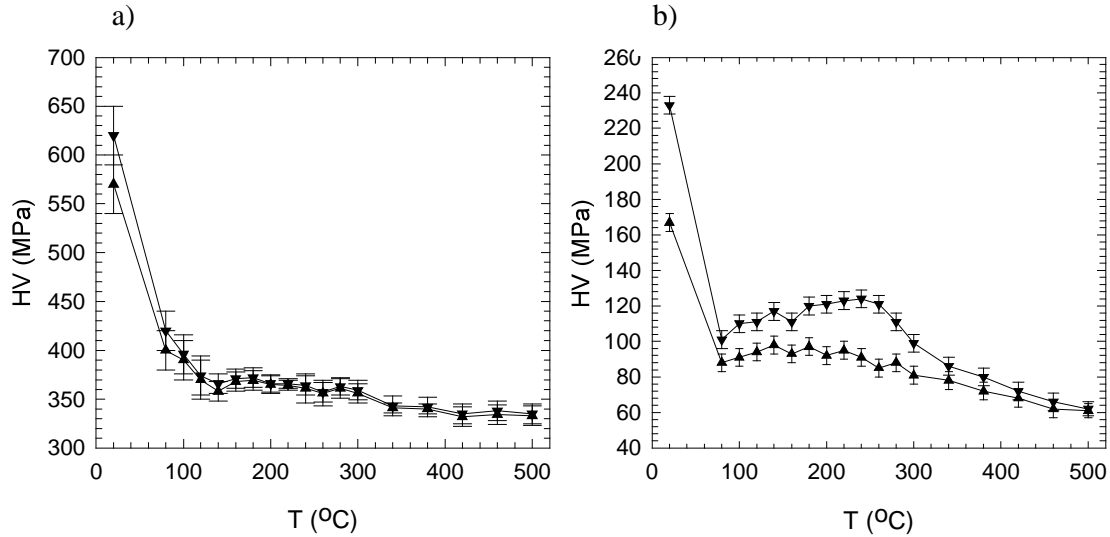


Figure 5: Temperature dependence of microhardness HV a) HPT deformed pure Mg, b) HPT deformed Mg10Gd. Maximum HV values (corresponding to the edge of the specimen) are plotted by triangles oriented down, while minimum HV values (corresponding to the center) are shown by triangles oriented up. Each point is a mean value from 10 different positions at the same radial distance r from the center.

Temperature dependence of the intensity I_2 of the dislocation component for HPT deformed Mg10Gd is plotted in Figure 4b, while Figure 5b shows microhardness, HV, of this sample as a function of the annealing temperature. Decomposition of supersaturated solid solution (sss) and precipitation effects in homogenized (i.e. coarse-grained) Mg10Gd alloy were studied in details elsewhere [2,10]. The decomposition takes place in the sequence $sss \rightarrow \beta''$ (D019) $\rightarrow \beta'$ (cbco) $\rightarrow \beta$ (Mg_5Gd , cubic).

The β'' and β' are metastable phases, while β formed at higher temperatures represents the stable phase. We have found in this work that the precipitation effects in HPT deformed Mg10Gd differ significantly from those in corresponding coarse-grained material. It is clear from Figure 4b that a radical decrease of I_2 occurs in the

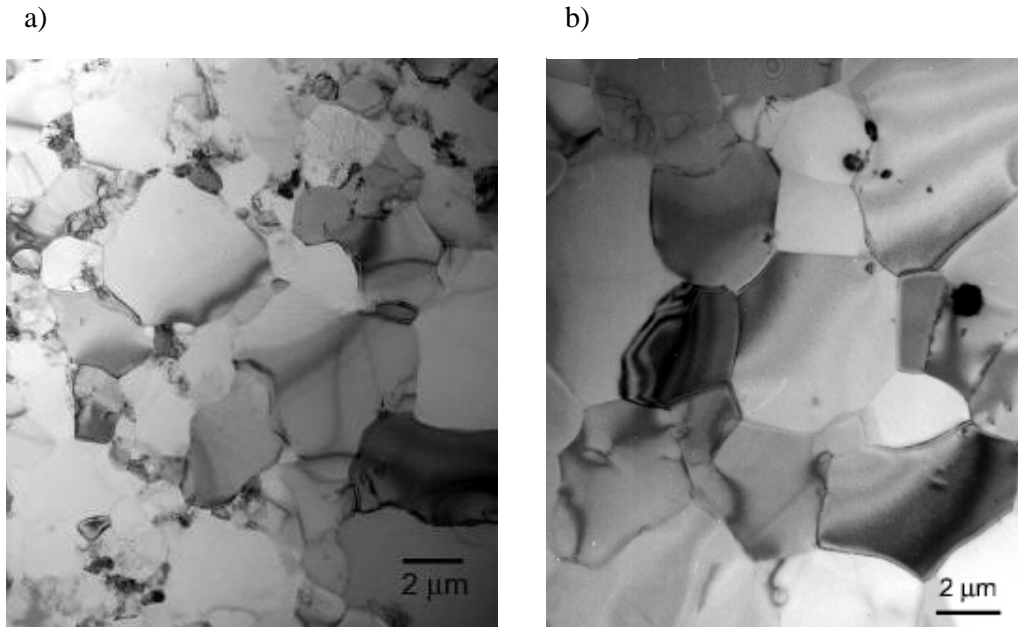


Figure 6: A bright field TEM image of HPT deformed Mg annealed up to a) 100 °C, b) 200°C.

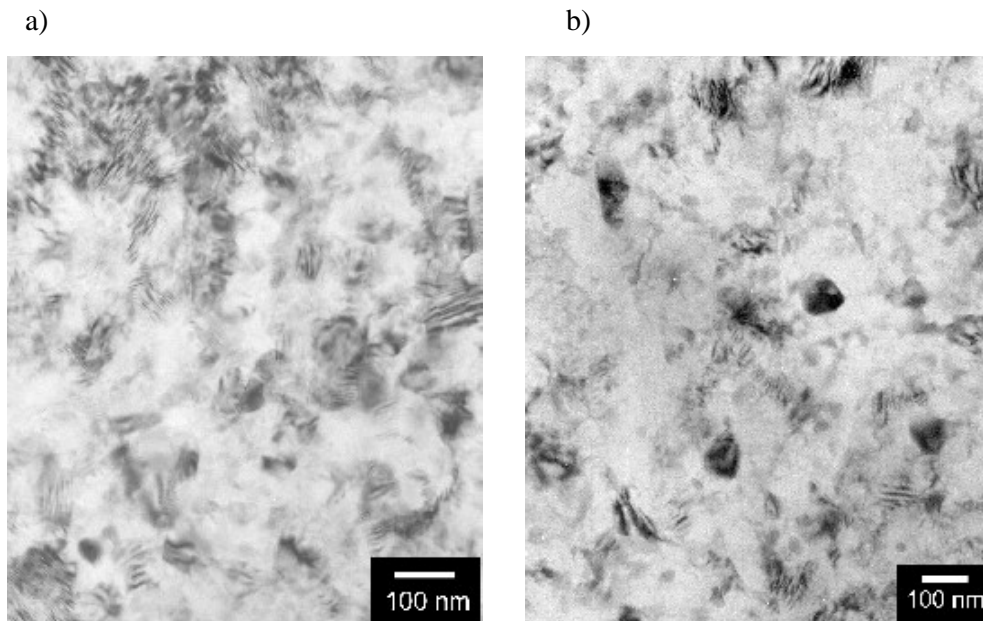


Figure 7: A bright field TEM image of HPT deformed Mg10Gd annealed up to a) 160 °C, b) 220°C.

temperature interval (100-240)°C in HPT deformed Mg10Gd sample. It directly indicates a significant recovery of dislocations in this temperature range. A slight local increase of I_2 at 100°C is likely due to formation of the β'' phase as confirmed by coincidence Doppler broadening [10]. However, the β'' phase particles are very fine (10 nm in diameter or less) because they were not observed by TEM. It should be noted that the high dislocation density makes TEM observations of fine precipitates very difficult. One can see from Figure 5b that HV exhibits an abrupt decrease after annealing to 80°C in HPT deformed Mg10Gd, i.e. there is a substantial softening, which occurs prior to the recovery of dislocations. It is probably due to a relaxation of stresses introduced into the sample by HPT. A bright field TEM image of HPT deformed Mg10Gd annealed up to 160 °C is shown in Figure 7a. One can see that the sample exhibits virtually the same UFG structure as in the as-deformed state (c.f. Figure 3b). Figure 7b shows TEM image of the sample annealed up to 220 °C. Despite the drastic decrease of I_2 at this temperature (see Figure 4b) no grain growth can be seen by TEM. There is certainly a decrease of dislocation

density reflected by a drop of I_2 but the grain size does not change. A bright field TEM image of HPT deformed Mg10Gd annealed up to 260°C is shown in Figure 8a. One can observe a significant decrease of dislocation density in grains. However, grain size does not increase and lies still around 100 nm. Thus, we can conclude that contrary to HPT deformed Mg, the recovery of dislocations in HPT deformed Mg10Gd is not accompanied by grain growth. We have found by TEM that the mean grain size remains around 100 nm up to $\approx 340^\circ\text{C}$, which demonstrates very good thermal stability of UFG structure in HPT deformed Mg10Gd. Annealing to temperatures higher than 340°C leads to recrystallization and a pronounced grain growth. It can be seen in Figure 8b which shows microstructure of HPT deformed Mg10Gd annealed up to 380 °C. A local maximum of I_2 at 300°C (see figure 4b) is due to precipitation of the equilibrium β phase. Positrons are trapped at the misfit defects between the incoherent β phase particles and the matrix. It results in a local increase of I_2 . The β phase precipitates were identified by TEM. Thus, contrary to the coarse-grained sample [10], precipitation of the metastable β' phase is omitted in HPT deformed Mg10Gd and the stable β phase is formed at significantly lower temperatures. Coarsening of the β phase particles causes subsequent decrease of I_2 , see Figure 4b. Above 450°C, the β phase particles dissolve and the solid solution is restored.

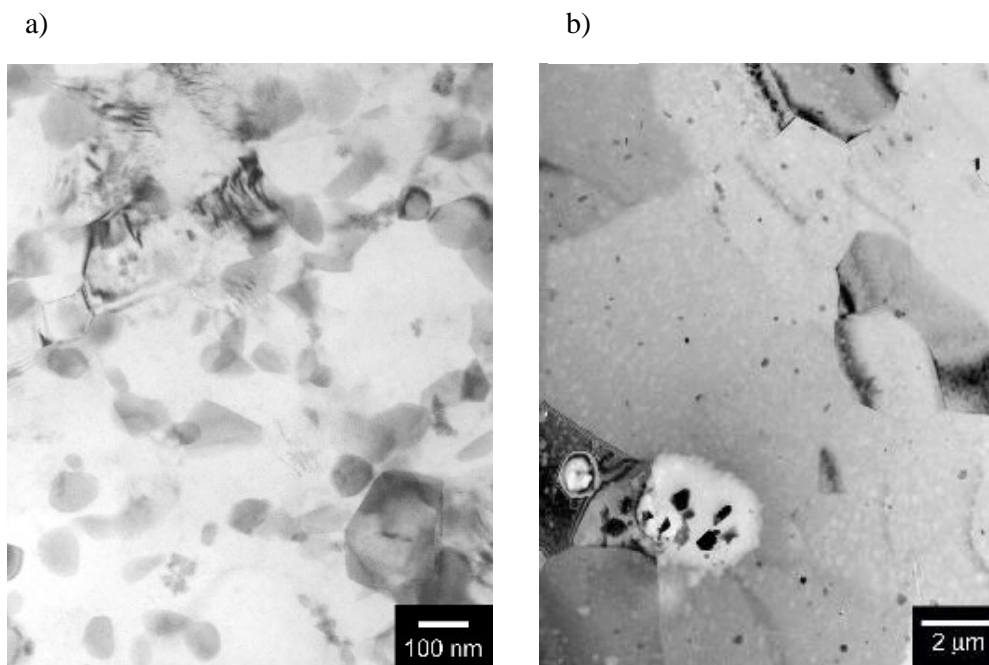


Figure 8: A bright field TEM image of HPT deformed Mg10Gd annealed up to a) 300 °C, b) 380°C.

Conclusions

The microstructure of HPT deformed Mg and Mg10Gd and its development with temperature were characterised. An incomplete dynamic recovery took place during HPT processing of Mg sample which resulted in a binomial type of structure. The HPT deformed Mg10Gd exhibits homogeneous UFG microstructure with high density of uniformly distributed dislocations and grain size about 100 nm. Recovery of dislocations starts already at room temperature in HPT deformed Mg and is accompanied by recrystallization. On the other hand, Mg10Gd exhibits a dramatic decrease of dislocation density in the temperature interval (100-240) °C, but no grain growth occurs in this temperature range. The mean grain size remains around 100 nm up to $\approx 340^\circ\text{C}$ in HPT deformed Mg10Gd. Formation of the metastable β' phase does not occur and the precipitation of the stable β phase is shifted to lower temperatures compared to the coarse grained alloy.

Acknowledgments

The work was financially supported by The Czech Science Foundation (contract 106/05/0073) and The Ministry of Education, Youth and Sports of Czech Republics (project MS 0021620834).

References

1. Mordike, B.L., "Creep-Resistant Magnesium Alloys," *Mat. Sci. Eng. A* **324**, 103-112 (2002).

2. Vostrý, P., Smola, B., Stulíková, I., von Buch, F., Mordike, B.L., "Microstructure Evolution in Isochronally Heat Treated Mg-Gd Alloys," *phys. stat. sol. (a)* **175**, 491-500 (1999).
3. Valiev, R.Z., Islamgaliev, R.K., Alexandrov, I.V., "Bulk Nanostructured Materials from Severe Plastic Deformation," *Prog. Mat. Sci.* **45**, 103-189 (2000).
4. Hautojärvi, P., Corbel, C., "Positron Spectroscopy of Defects in Metals and Semiconductors," in *Proceedings of the International School of Physics "Enrico Fermi", Course CXXV* (Eds. Dupasquier, A., Mills, A.P.), IOS Press, Varena, pp. 491-532 (1999).
5. Bečvář, F., Čížek, J., Lešťák, L., Novotný, I., Procházka, I., Šebesta, F., "A High-Resolution BaF₂ Positron-Lifetime Spectrometer and Experience with Its Long-Term Exploitationm," *Nucl. Instr. Meth. A* **443** 557-577 (2000) .
6. Procházka, I., Novotný, I., Bečvář, F., "Application of Maximum-Likelihood Method to Decomposition of Positron-Lifetime Spectra to Finite Number of Components," *Mat. Sci. Forum* **225-257** 772-774 (1997).
7. Puska, M.J., Nieminen, R.N., "Defect Spectroscopy with Positrons – a General Computational Method," *J. Phys. F: Met. Phys.* **13**, 333-346 (1983).
8. Čížek, J., Procházka, I., Brauer, G., Anwand, W., Kužel, R., Cieslar, M., Islamgaliev, R.K., "Spatial Distribution of Defects in Ultra-Fine Grained Copper Prepared by High-Pressure Torsion," *phys. stat. sol. (a)* **195**, 335-349 (2003).
9. Fahnle, M., Meyer, B., Mayer, J., Oehrens, J.S., Bester, G., "Diffusion Mechanisms in Crystalline Materials," (Ed. Mishin, Y.) *MRS Symposia Proceedings No. 527*, pp. 23-31 (1987).
10. Čížek, J., Procházka, I., Bečvář, F., Stulíková, I., Smola, B., Kužel, R., Cherkaska, V., Islamgaliev, R.K., Kulyasova, O., "Thermal Development of Microstructure and Precipitation Effects in Mg-10wt.%Gd Alloy," *phys. stat. sol. (a)* (2005) submitted for publication.
11. Čížek, J., Procházka, I., Cieslar, M., Kužel, R., Kuriplach, J., Chmelík, F., Stulíková, I., Bečvář, F., Melikhova, O., Islamgaliev, R.K., "Thermal Stability of Ultrafine Grained Copper," *Phys. Rev. B* **65**, 094106 (2002).
12. Čížek, J., Procházka, I., Cieslar, M., Stulíková, I., Chmelík, F., Islamgaliev, R.K., "Positron-Lifetime Investigation of Thermal Stability of Ultra-Fine Grained Nickel," *phys. stat. sol. (a)* **191**, 391-408 (2002).